JMEPEG (2011) 20:1512–1519
DOI: 10.1007/s11665-011-9856-9

1059-9495/$19.00

A Physically Consistent Path-Weighted Diffusivity Function for Modeling of Drop-by-Drop Liquid Metal Deposition

S.G. Lambrakos and K.P. Cooper

(Submitted October 28, 2010)

A physically consistent path-weighted diffusivity function is derived for parametric representation of heat diffusion patterns occurring within a volume of material where in there exists inhomogeneous or anisotropic thermal diffusivity. A physically consistent parametric representation of energy deposition processes, where there exists spatially dependent thermal diffusivity, provides for more optimal inverse analysis of such processes. The path-weighted diffusivity function presented here further extends an inverse analysis approach presented previously. The general functional characteristics of the path-weighted diffusivity function derived are examined via a prototype simulation of drop-by-drop liquid metal deposition upon a material characterized by anisotropic thermal diffusivity. The results of this simulation are compared with previous simulations concerning path-weighted thermal diffusivity. The parametric representations presented, which are constructed using path-weighted sums of analytic basis functions, are examined from the perspective of discrete numerical methods. This perspective provides a foundation for the development of control algorithms for process optimization with respect to achieving specific microstructures within a fabricated structure.

Keywords fabricated metal, modeling processes, shaping

1. Introduction

The inverse analysis of energy deposition processes requires parametric representations that are both conveniently adjustable and physically consistent with the nature of these processes. For the inverse analysis of processes involving drop-by-drop liquid-metal deposition (Ref 1-4), where there can exist spatially dependent thermal diffusion, parametric representations that are in terms of path-weighted diffusivity functions should be more appropriate (Ref 5). It follows that a physically consistent path-weighted diffusivity function provides for a more optimal parametric representation of spatially dependent thermal diffusion.

A physically consistent path-weighted diffusivity function is derived for parametric representation of heat diffusion patterns occurring within a volume of material where in there exists inhomogeneous or anisotropic thermal diffusivity. A physically consistent parametric representation of energy deposition processes, where there exists spatially dependent thermal diffusivity, provides for more convenient inverse analysis of such processes. The path-weighted diffusivity function presented in this article further extends an inverse analysis approach presented previously (Ref 6, 7). This approach is based on the use of parametric representations that are constructed according to the following concepts, which have been discussed previously (Ref 6, 7). These concepts are the use of generalized functions, parameterizations in terms of basis functions, general trend characteristics of energy deposition, energy source functions, and parameterizations for modulation of heat diffusion patterns. Considered in this article are parametric representations of heat diffusion patterns occurring within a volume of material where in there exists inhomogeneous or anisotropic thermal diffusivity. These parameterizations are formulated in terms of path-weighted diffusivity functions.

The organization of the subject areas presented in this article are as follows. First, a brief review is given of the inverse heat deposition problem and of its specific definition for the analysis method considered. Second, parametric representations are constructed for spatial modulation of heat diffusion patterns that use path-weighted sums of analytic basis functions. It is with respect to the formal structure of these basis functions that a physically consistent path-weighted diffusivity function is derived. Third, a prototype analysis is presented for the purpose of examining the functional characteristics of the parametric representation, which is defined in terms of a path-weighted diffusivity function. This analysis provides a demonstration of the effectiveness of the parametric representation presented for modeling processes involving drop-by-drop liquid metal deposition. Fourth, the parametric representations, which are constructed using path-weighted sums of analytic basis functions, are examined from the perspective of discrete numerical methods and control algorithms for process optimization with respect to specific microstructures. Finally, a conclusion is given.

S.G. Lambrakos and **K.P. Cooper**, Materials Science and Technology Division, Code 6390, Naval Research Laboratory, Washington, DC 20375-5320. Contact e-mails: lambrakos@nrl.navy.mil.

2. The Inverse Heat Deposition Problem

The inverse problem concerning analysis of processes involving heat transfer may be stated formally in terms of

source functions (or input quantities) and multidimensional temperature fields (output quantities). The inverse problem given in this article is focused on the determination of heat fluxes in materials having inhomogeneous or anisotropic thermal diffusivity, i.e., a spatially dependent diffusivity function.

Following the inverse analysis approach, a parametric representation based on a physical model provides a means for the inclusion of information concerning the physical characteristics of a given energy deposition process. It follows then that for heat deposition processes involving the deposition of heat within a bounded region of finite volume, consistent parametric representations of the temperature field are given by

$$T(\hat{x},t,\kappa) = T_{\mathrm{A}} + \sum_{k=1}^{N_k} T_k(\hat{x},\hat{x}_k,t,\kappa) \quad \text{and} \quad T(\hat{x}_n^{\mathrm{c}},t_n^{\mathrm{c}},\kappa) = T_n^{\mathrm{c}} \tag{Eq 1}$$

where the quantity T_{A} is the ambient temperature of the workpiece and the locations $\hat{x}_n^{\mathrm{c}}$ and temperature values T_n^{c} specify constraint conditions on the temperature field. The functions $T_k(\hat{x},\hat{x}_k,t,\kappa)$ represent an optimal basis set of functions for given sets of boundary conditions and material properties. The quantities $\hat{x}_k = (x_k, y_k, z_k)$, $k = 1,\ldots,N_k$, are the locations of the elemental source or boundary elements.

Although heat deposition processes may be characterized by complex coupling between the heat source and workpiece, as well as complex geometries associated with either the workpiece or deposition process, in terms of inverse analysis, the general functional forms of the temperature fields associated with all such processes are within a restricted class of functions, i.e., optimal sets of functions. Accordingly, a sufficiently optimal set of functions is that of analytic solutions to heat conduction equation for a finite set of boundary conditions (Ref 8). A parameterization based on this set is both sufficiently general and convenient relative to optimization.

The formal procedure underlying the inverse method considered entails the adjustment of the temperature field defined over the entire spatial region of the sample volume at a given time t. This approach defines an optimization procedure where in the temperature field spanning the spatial region of the sample volume is adopted as the quantity to be optimized. The constraint conditions are imposed on the temperature field spanning the bounded spatial domain of the workpiece by minimization of the value of the objective functions defined by

$$Z_{\mathrm{T}} = \sum_{n=1}^{N} w_n \left(T(\hat{x}_n^{\mathrm{c}},t_n^{\mathrm{c}},\kappa) - T_n^{\mathrm{c}}\right)^2 \tag{Eq 2}$$

where T_n^{c} is the target temperature for position $\hat{x}_n^{\mathrm{c}} = (x_n^{\mathrm{c}}, y_n^{\mathrm{c}}, z_n^{\mathrm{c}})$.

The input of information into the inverse model defined by Eq 1 and 2 is effected by the assignment of individual constraint values to the quantities T_n^c; the form of the basis functions adopted for parametric representation; and specifying the shapes of the inner and outer boundaries, S_{i} and S_{o}, respectively, which bound the temperature field within a specified region of the workpiece.

At this point, it is significant to note the following. First, the general trend features of heat deposition processes are such that the construction of a complete basis set of functions $T_k(\hat{x},\hat{x}_k,t,\kappa)$ making up a linear combination of the form defined by Eq 1 for representation of the associated temperature field is well defined and readily achievable. Second, for heat deposition processes, characteristics of the temperature field are poorly correlated to characteristics of the energy source. The characteristics of the temperature field that are associated with these processes, however, are strongly coupled only to inner boundaries on this field, e.g., the solidification boundary. This property follows from the low-pass spatial filtering property of the basis functions, $T_k(\hat{x},\hat{x}_k,t,\kappa)$, whose general forms are consistent with the dominant trend features of heat deposition processes (see Ref 6). Third, given a consistent set of basis functions, the temperature field associated with a heat deposition process is completely specified by the shape and temperature distribution of a given inner boundary on the domain of the temperature field; the diffusivity κ and speed of deposition V; and the lengths of the spatial dimensions $\{D_{\mathrm{i}}\}$of the workpiece. Fourth, the shape and temperature distribution of a specified inner boundary S_{i} is determined by the rate of energy deposited on the surface of the workpiece and the strength of coupling of the energy source to the workpiece. And finally, in that an inner boundary S_{i} is defined by its shape and the distribution of temperatures on its surface $T(\hat{x}_{\mathrm{S}})$, it follows that one can define a multidimensional temperature field $T(\hat{x}, \kappa, V, \{D_{\mathrm{i}}\}, T(\hat{x}_{\mathrm{S}})$, and $\hat{x}_{\mathrm{S}} \in S_{\mathrm{i}})$.

3. Analytic Basis Functions and Path-Weighted Diffusivity Functions

As demonstrated in previous studies, the parametric representation of the form given by Eq 1 is sufficiently flexible for construction of temperature fields associated with heat deposition processes where source and workpiece characteristics are relatively simple. It is significant to note, however, that many energy deposition processes are characterized by volumetric coupling of the energy source and associated diffusion patterns that are relatively complex. Accordingly, it would be advantageous to extend the adjustability of the mapping defined by Eq 1 for the purpose of representing more complex diffusion patterns. As shown above, the adjustability of the parameterization can be extended by adopting basis functions whose spatial distributions are spatially modulated. Among the many different possible types of spatial modulation that can be applied are those whose application produces diffusion patterns that are directionally or path weighted.

Given the parameterization framework defined by Eq 1 and 2, it follows that consistent representations, in terms of basis functions, of the temperature field associated with spatially modulated heat diffusion patterns are

$$T(\hat{x},t) = T_{\mathrm{A}} + \sum_{k=1}^{N_k}\sum_{n=1}^{N_t} C(\hat{x}_k) F(\hat{x},\hat{x}_k,n\Delta t,\langle\kappa(\hat{x})\rangle)\delta(n\Delta t - t_k) \tag{Eq 3}$$

where

$$F(\hat{x},\hat{x}_k,t,\langle\kappa(\hat{x})\rangle) = \frac{1}{t}\exp\left[-\frac{(x-x_k)^2+(y-y_k)^2}{4\langle\kappa(\hat{x})\rangle t}\right] \times \left\{1 + 2\sum_{m=1}^{\infty}\exp\left[-\frac{\langle\kappa(\hat{x})\rangle m^2\pi^2 t}{l^2}\right]\cos\left[\frac{m\pi z}{l}\right]\cos\left[\frac{m\pi z_k}{l}\right]\right\}, \tag{Eq 4a}$$

or

$$F(\hat{x},\hat{x}_k,t,\langle\kappa(\hat{x})\rangle)=\frac{1}{t^{3/2}}\exp\left[-\frac{(x-x_k)^2+(y-y_k)^2+(z-z_k)^2}{4\langle\kappa(\hat{x})\rangle t}\right] \quad \text{(Eq 4b)}$$

where $t=N_t\Delta t$ and $\delta(t-t_k)$ is the Dirac delta function representing the instantaneous deposition at locations $\hat{x}_k=(x_k, y_k, z_k)$ at times $t=t_k$. The speed of energy deposition V_k, which is an implicit function of position on the surface of the workpiece, is given by

$$V_k=\frac{x_k-x_{k-1}}{t_k-t_{k-1}}. \quad \text{(Eq 5)}$$

Referring to Eq 3-5, it is to be noted that spatial modulation of the diffusion field is through functional dependence on the path-weighted diffusivity function $\langle\kappa(\hat{x})\rangle$. Accordingly, the procedure for inverse analysis defined by Eq 1-5 entails adjustment of the parameters $C(\hat{x}_k)$, $\hat{x}_k$, Δt, and V_k, defined over the entire spatial region of the workpiece, and specification of the function $\langle\kappa(\hat{x})\rangle$. With respect to inverse analysis, the only condition on the form of $\langle\kappa(\hat{x})\rangle$ is that it be consistent with the general trend features of anisotropic diffusivity. The goal of using a reasonably optimal set of basis functions for parametric representation, however, implies the necessity of adopting a form of $\langle\kappa(\hat{x})\rangle$ that is physically consistent with heat diffusion occurring within materials having anisotropic diffusivity.

At this point, it is significant to note that a physically consistent path-weighted diffusivity function can be derived with respect to the formal structure of Eq 4. The formal structure of Eq 4 implies that a more physically consistent path-weighted diffusivity function is with respect to path integration of the inverse of the square root of diffusivity function, i.e., $1/\sqrt{\kappa}$, and therefore that a quantity $\langle\kappa_m\rangle$ can be defined by the expression

$$\left\langle\frac{1}{\sqrt{\kappa(r,\theta)}}\right\rangle=\frac{1}{r}\int_0^r\frac{dr'}{\sqrt{\kappa(r',\theta)}}\approx\frac{1}{2}\left[\frac{1}{\sqrt{\kappa(0,\theta)}}+\frac{1}{\sqrt{\kappa(r,\theta)}}\right]. \quad \text{(Eq 6)}$$

Next, given that the origins of the discrete paths are associated with the discrete source distribution $C(\hat{x}_k)$, it follows from Eq 6 that

$$\langle\kappa_m(\hat{x}_k,\hat{x})\rangle=\frac{4\kappa(\hat{x}_k)\kappa(\hat{x})}{\left(\sqrt{\kappa(\hat{x}_k)}+\sqrt{\kappa(\hat{x})}\right)^2} \quad \text{(Eq 7)}$$

where the directional path-weighting defined by Eq 7 represents a path-integral mean value, and the directional tracking of diffusivity values at near-neighbor locations is not required.

4. Prototype Analysis

In this section, prototype calculations are presented, which consider energy deposition within a material characterized by inhomogeneous and anisotropic thermal diffusivity. These calculations demonstrate the functional characteristics of the path-weighted diffusivity function, Eq 7. The prototype system is that of the freeform fabrication of a two-dimensional coupon for a system whose thermal diffusivity is a function of position.

Table 1 Model parameters used to determine thermal fields in droplet-by-droplet deposition process

Model parameters
Material: Cu-Ni Alloy distribution
Diffusivity: Given by Eq 7
Timestep: Δt = 0.005 s
Drop deposited every 5 time-steps
11 drops per layer
Droplet energy content: $C(\hat{x}_k)$ = 4.0
Droplet volume = $(\Delta l)^3$, Δl = 0.1667 cm

The model system consists of a sequence of layers, where each layer consists of a distribution of discrete energy sources whose strengths are assigned by the values of the coefficients $C(\hat{x}_k)$ defined in Eq 3 and are numerically integrated, or summed discretely, at each time-step. Each of the discrete energy sources represents a discrete liquid-metal droplet of a given volume. The translation speed of the sample relative to the point of liquid-metal deposition is assigned implicitly through the time dependence and relative locations of the discrete energy sources, $C(\hat{x}_k)$. That is to say, a certain number of drops per layer and a certain number of layers as a function of time are specified. The model parameters used for the prototype analysis are listed in Table 1. For purposes of this analysis, the basis function $F(\hat{x},\hat{x}_k,t,\kappa)$ given by Eq 4a is adopted for calculation of the temperature field. These functions are the solution to the heat conduction equation for a temperature-independent diffusivity and non-conducting boundaries on two surfaces that are separated by a distance l, which for this simulation is sufficiently large that the influence of one boundary can be neglected. Accordingly, it is assumed for this simulation that there is no conduction at the substrate boundary. An additional condition imposed on the model system is that of heat transfer into the ambient environment at the edges of the rectangular coupon being fabricated. This is a realistic assumption for process conditions where droplet-by-droplet deposition occurs within a mold structure consisting of a metal powder composite whose thermal diffusivity is similar to that of the fabricated structure, e.g., rectangular coupon. A constraint condition imposed on the temperature field is that the liquid-solid interface defined by the alloy liquidus temperature is at that of the specific alloy at any given position within the material. Accordingly, the values assigned to the coefficients $C(\hat{x}_k)$ were such that the average temperature of each discrete droplet was within the range of liquid metal. It is significant to note that other constraint conditions, such as melt pool dimensions and measurements of temperature via thermocouples, can also be adopted for assigning values to the coefficients $C(\hat{x}_k)$. In the present prototype analysis, the layers are deposited one on top of the other by traversing the passes in a zig-zag fashion. Consistent with the filter properties associated with thermal diffusion, each melt bead droplet can be represented by a cube (see Table 1). This follows in that the filtering of fine spatial structure, which is due to the Fourier transform character of Eq 4, implies that the temperature field is insensitive to details of the shape of the melt bead droplet. It is significant to note, however, that the temperature field is sensitive to the spatial distribution of droplets. The prototype analysis considers calculation of the temperature field at three different sampling points within the model structure.

The prototype analysis is characterized by energy deposition within a material having inhomogeneous and anisotropic thermal diffusivities. The system, which consists of a two-dimensional discrete distribution of Cu-Ni alloys of variable relative percentages as a function of position, is described schematically in Fig. 1. This alloy distribution is characteristic of that which would be constructed by drop-by-drop liquid metal deposition of 11 alloys (differing in wt.%) being dropped sequentially to build up a thin wall. For this system, the liquidus temperature is also a function of relative alloy composition. A diffusivity function and average liquidus temperature field are constructed according to the two-dimensional discrete distribution of Cu-Ni alloys. Accordingly,

$$\kappa_m(x,y,z) = (1 - x/L)\kappa_1 + (x/L)\kappa_2 \quad \text{and} \quad T_{\mathrm{M}}(x,y,z) = (1 - x/L)T_{\mathrm{M1}} + (x/L)T_{\mathrm{M2}} \qquad \text{(Eq 8)}$$

where $\kappa_1 = 1.136 \times 10^{-4}\,\mathrm{m}^2/\mathrm{s}$, and $T_{\mathrm{M1}} = 1085$ °C, corresponding to pure Copper, and $\kappa_2 = 2.303 \times 10^{-4}\,\mathrm{m}^2/\mathrm{s}$, and $T_{\mathrm{M2}} = 1455$ °C, corresponding to pure Nickel. The prototype analysis that follows consists of temperature field calculations that demonstrate the influence of path-weighted diffusivity on heat diffusion patterns according to adjustment of the various parameters associated with the basis functions defined by Eq 3-7. Considered are calculations of temperature fields which adopt the spatially dependent diffusivity function Eq 8, the constant diffusivities $\kappa_1 = 1.136 \times 10^{-4}\,\mathrm{m}^2/\mathrm{s}$ and $\kappa_2 = 2.303 \times 10^{-4}\,\mathrm{m}^2/\mathrm{s}$, corresponding to pure Copper and Nickel, respectively, and discrete spatial distributions of the effective heat sources $C(\hat{x}_k)$ defined by Eq 3. The distribution $C(\hat{x}_k)$ is adjusted so that the calculated cross sections of the solidification boundary satisfy, in principle, the experimentally observed solidification patterns or droplets of given volume, whose average temperature (above liquidus) has been specified. The results of these calculations are shown in Fig. 3 for the weighted sums of basis functions defined by Eq 7.

An example for the potential application of the two-dimensional model adopted for prototype analysis here is shown in Fig. 1(b), which is that of the fabrication of a turbine blade by laser melt-deposition (Ref 9). It can be seen from this figure that the aspect ratio defined by the thickness of this structure relative to its other dimensions is such that heat transfer is essentially two-dimensional in character.

Shown in Fig. 2(a)-(c) is the time-dependent temperature field at different stages of the droplet-by-droplet liquid metal deposition processes during the formation of a structure consisting of five layers according to the sequence defined by Fig. 1(a). Referring to these figures, one can establish a visual correlation of the temperature history at any given sampling point with the relative position of the liquid metal droplet at the time of deposition. Accordingly, the temperature histories at the sampling points indicated in Fig. 1(a) can be examined relative to the position of the liquid metal droplet of pure Cu, pure Ni, or Cu-Ni alloy composite at different stages of the droplet sequence. The results of this type of calculation are shown in Fig. 3-5.

4.1 Discussion

At this point, the calculations shown in Fig. 3-5 are examined with respect to the inverse analysis formalism defined above. Referring to these figures, one can associate the boundary defined by the liquidus temperature (see Fig. 2) with an inner boundary S_{i}, and similarly, the temperature history shown in Fig. 4 with a point on the surface of an outer boundary S_{o}. It is significant to note that, in principle, temperatures associated with both S_{i} and S_{o} are experimentally observable and therefore adoptable as constraints for application of the procedure defined by Eq 1 and 2.

An interesting qualitative result of the calculations shown in Fig. 3-5 is that they demonstrate reasonable sensitivity of temperature histories to alloy distribution within a material. This implies that an alloy distribution can be, in principle, adopted as a process parameter for control of temperature history, as well as, droplet size and energy content. Control of temperature history would imply, in turn, control of microstructure within a structure that is built by means of drop-by-drop metal deposition.

Physical consistency of the path-weighted diffusivity is demonstrated with reference to the temperature history corresponding to Cu-Ni alloy composite shown in Fig. 3-5. Referring to Fig. 3, it can be seen that the temperature history of the Cu-Ni alloy composite tracks very closely, and has as an upper bound, the temperature history of the pure Ni system. Similarly, referring to Fig. 5, that the

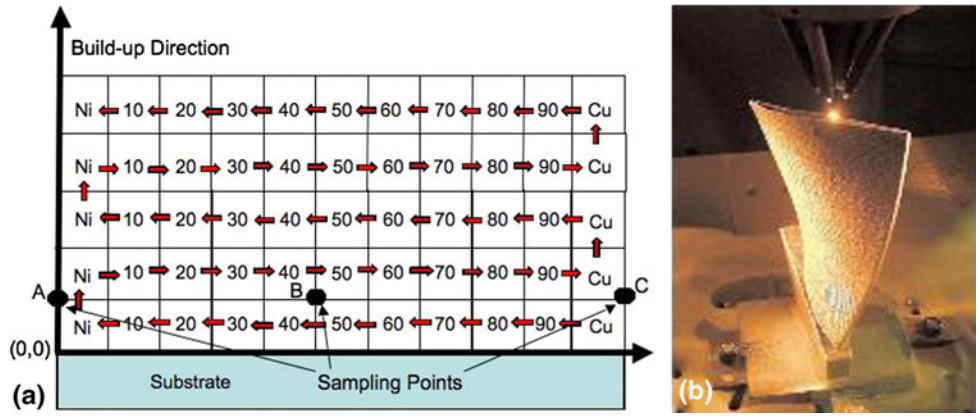

Fig. 1 (a) Schematic representation of drop-by-drop liquid metal deposition process assumed for construction of five layer two-dimensional structure. Sampling points A, B and C are at locations $(0, 10\Delta l)$, $(90\Delta l, 10\Delta l)$ and $(190\Delta l, 10\Delta l)$, respectively, where $\Delta l = 0.1667$ cm. (b) A turbine blade being made by laser melt-deposition (Ref 9)

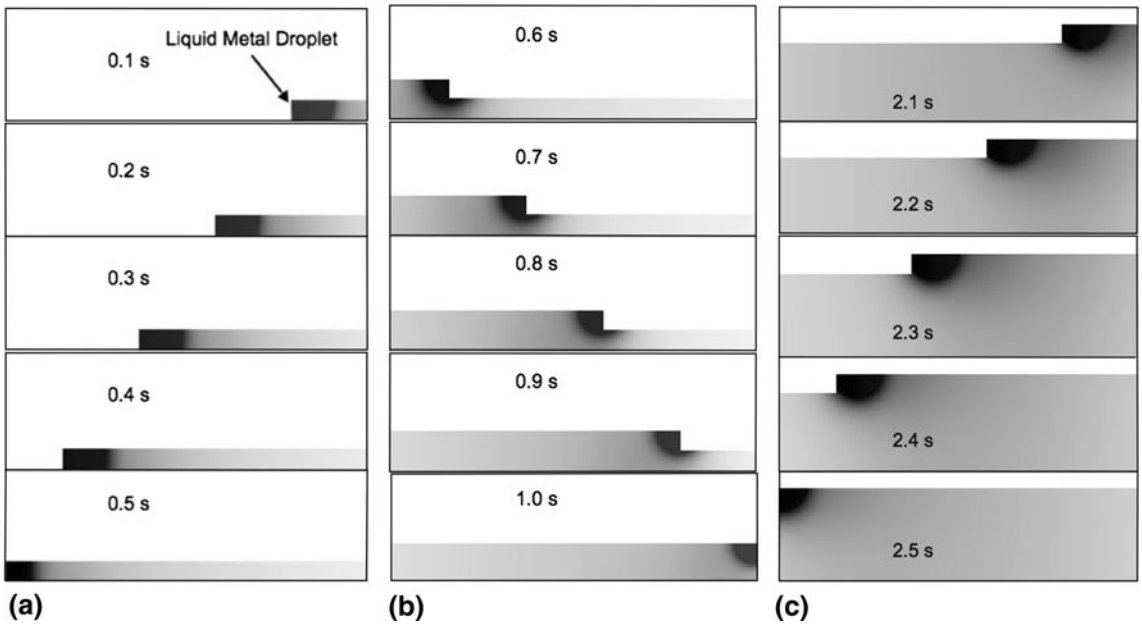

Fig. 2 (a) Time-dependent temperature field (°C) of two-dimensional built structure representing formation of first layer consisting of either pure Cu, pure Ni or Cu-Ni alloy composite. (b) Time-dependent temperature field (°C) of two-dimensional built structure representing formation of second layer consisting of either pure Cu, pure Ni or Cu-Ni alloy composite. (c) Time-dependent temperature field (°C) of two-dimensional built structure representing formation of fifth layer consisting of either pure Cu, pure Ni or Cu-Ni alloy composite. (d) Temperature field gray scale from 0 to 1455 °C for (a)-(c)

temperature history of the alloy composite tracks very closely, and has as an lower bound, the temperature history of the pure Ni system. The tracking of temperature histories in Fig. 3 and 5 is consistent with the large relative fractions of Ni and Cu, respectively. It can be seen from Fig. 4, the temperature history of the alloy composite is essentially the average of the temperature histories of the Cu and Ni systems. The is consistent with the relative fractions of Cu and Ni, which are close in value, at the sampling point considered.

Next, we examine the sensitivity of the calculated temperature fields with respect to the form of the path-weighted diffusivity functions. For this purpose, the same boundary conditions used in a previous study (Ref 5) are adopted for the present prototype analysis. Reference 5 presents an analysis of the same alloy composite system considered here, but considers a path-weighted diffusivity function that is with respect to path integration of the inverse of diffusivity function, i.e., $1/\kappa$. It is interesting to note that for both analyses, that in Ref 5 and here, the temperature histories of the Cu-Ni alloy composite, at a sampling point where the relative percentages of Cu and Ni are essentially the same (e.g., sampling point B in Fig. 2a), are essentially the average of the temperature histories of the Cu and Ni systems. This implies that path-weighting with respect to diffusivity is sensitive to average changes in values of the diffusivity, i.e., monotonic increases or decreases in value, but relatively insensitive to the detailed characteristics of the variation of diffusivity as a function of position. This insensitivity implies certain benefits with respect to the construction of discrete numerical methods for calculating time-dependent temperature histories. This issue is discussed further, in what follows, within the context of examining the parametric representation defined by Eq 3-5 from the perspective of discrete numerical methods and control algorithms for process optimization.

5. Numerical Methods for Modeling Drop-by-Drop

5.1 Liquid-Metal Deposition

The starting point for the construction of a numerical method for calculating time-dependent temperature histories for any given energy deposition process is a discrete representation of the heat conduction equation. In terms of finite differences, discrete representations of this equation, for calculation of timed-dependent temperature fields, fall within two classes, explicit or implicit schemes (see Ref 10 for further discussion). These classes are defined according to numerical stability conditions which determine the nature of error propagation as a function of time. Explicit schemes are characterized by relatively strict stability conditions on the choice of discrete time-step size. Implicit schemes are characterized by unconditional stability with respect to time-step size. With respect to explicit schemes, owing to a well-defined criterion for numerical stability, there exists an a priori measure, or rather sense, of error propagation within the calculated temperature fields as a function of time. This a priori measure of accuracy for calculated temperature fields comes at the very high price of very small time-step sizes, which renders many heat-transfer problems intractable with respect to numerical simulation via explicit schemes. Implicit schemes, owing to their unconditional stability with respect to time-step size, are well posed for numerical simulations of heat transfer over time and space scales that are of practical significance relative to process modeling. In general, however, it is difficult to access the accuracy of these schemes in that there does not exist rigorous criteria for error propagation. Typically, implicit schemes for discrete representation of the heat conduction equation are structured in terms of linear-algebraic formulations. These formulations provide a framework for the construction of various types of algorithms for purposes of numerical simulation.

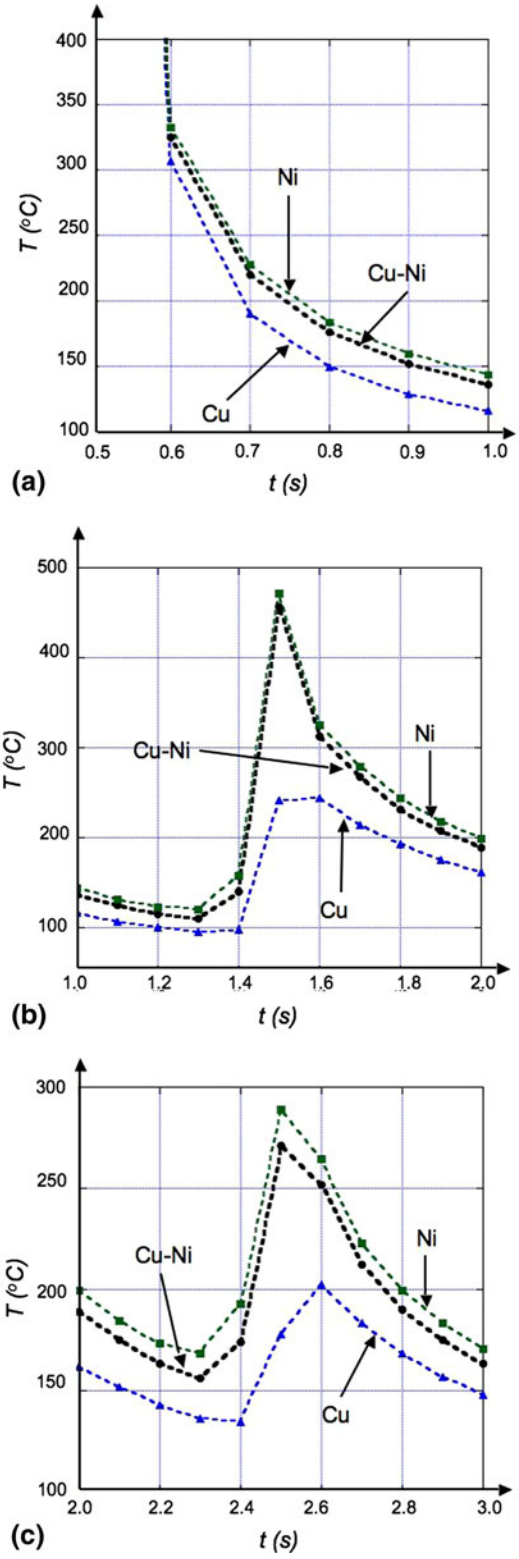

Fig. 3 (a) Temperature histories at sampling point A shown in Fig. 1 within two-dimensional built structures consisting of pure Cu, Pure Ni and Cu-Ni alloy composite for time period 0.5-1.0 s. (b) Temperature histories at sampling point A shown in Fig. 1 within two-dimensional built structures consisting of pure Cu, Pure Ni and Cu-Ni alloy composite for time period 1.0-2.0 s. (c) Temperature histories at sampling point A shown in Fig. 1 within two-dimensional built structures consisting of pure Cu, Pure Ni and Cu-Ni alloy composite for time period 2.0-3.0 s

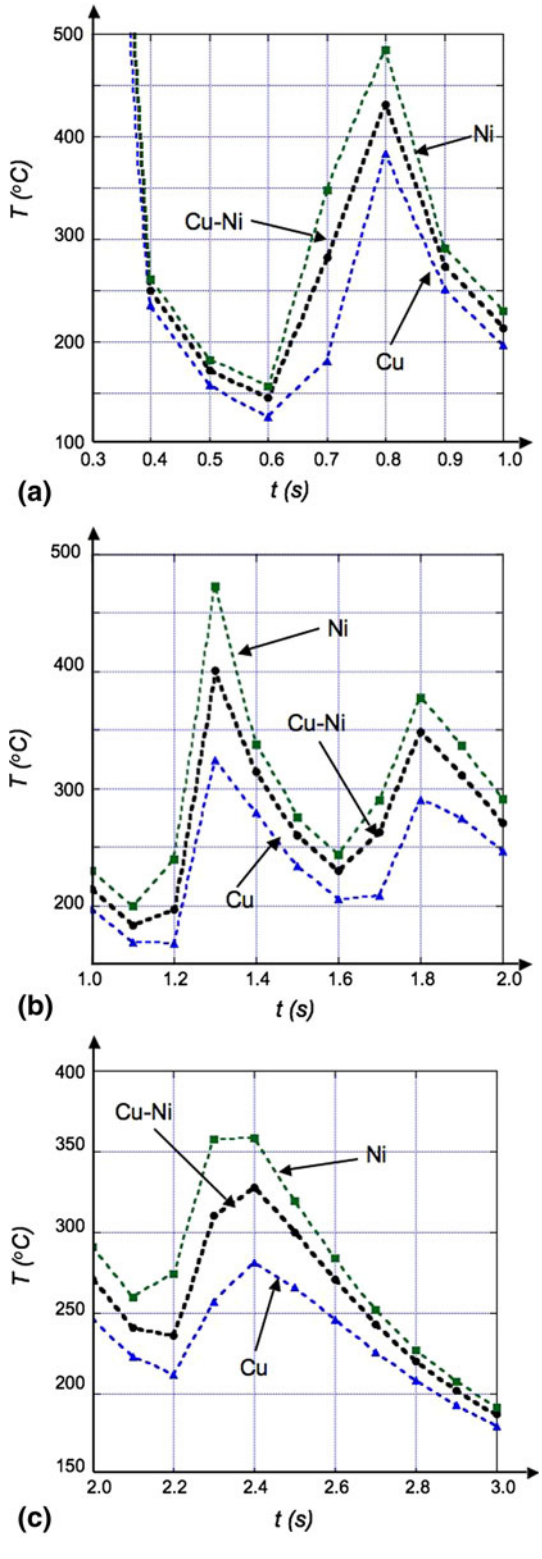

Fig. 4 (a) Temperature histories at sampling point B shown in Fig. 1 within two-dimensional built structures consisting of pure Cu, Pure Ni and Cu-Ni alloy composite for time period 0.3-1.0 s. (b) Temperature histories at sampling point B shown in Fig. 1 within two-dimensional built structures consisting of pure Cu, Pure Ni and Cu-Ni alloy composite for time period 1.0-2.0 s. (c) Temperature histories at sampling point B shown in Fig. 1 within two-dimensional built structures consisting of pure Cu, Pure Ni and Cu-Ni alloy composite for time period 2.0-3.0 s

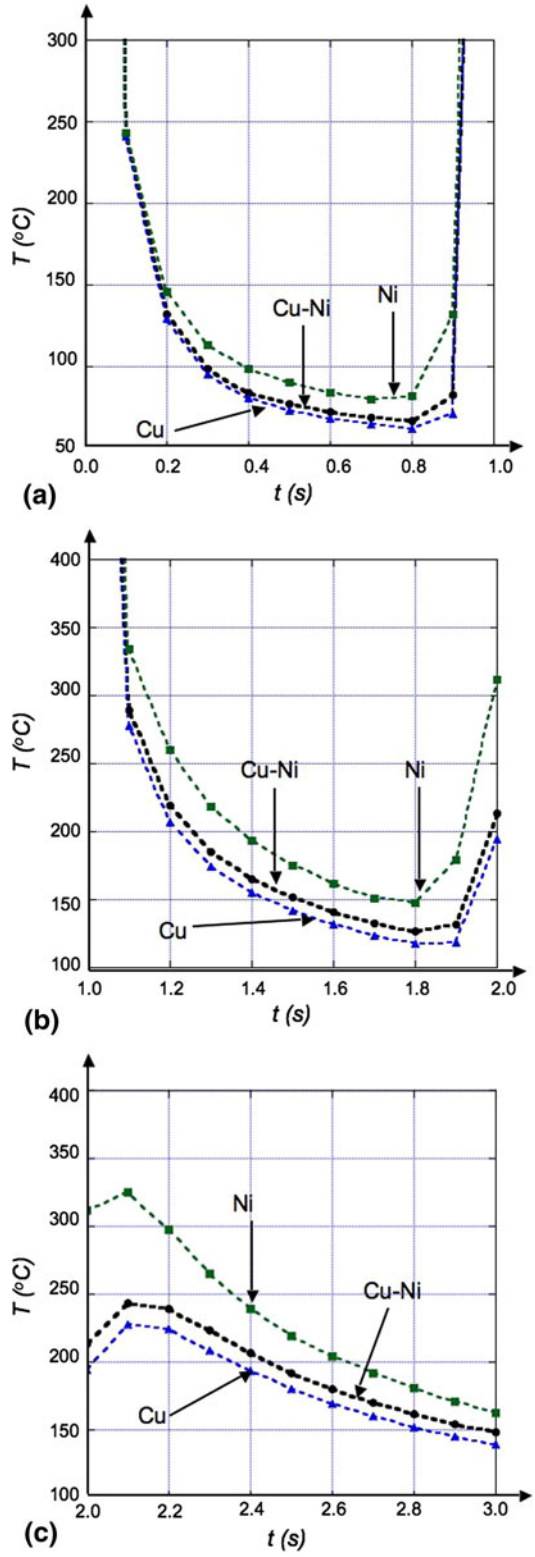

Fig. 5 (a) Temperature histories at sampling point C shown in Fig. 1 within two-dimensional built structures consisting of pure Cu, Pure Ni and Cu-Ni alloy composite for time period 0.0-1.0 s. (b) Temperature histories at sampling point C shown in Fig. 1 within two-dimensional built structures consisting of pure Cu, Pure Ni and Cu-Ni alloy composite for time period 1.0-2.0 s. (c) Temperature histories at sampling point C shown in Fig. 1 within two-dimensional built structures consisting of pure Cu, Pure Ni and Cu-Ni alloy composite for time period 2.0-3.0 s

It follows that, in terms of the classification of discrete representations of the heat conduction equation, the parametric representations Eq 3-5, which are constructed using path-weighted sums of analytic basis functions, provide an unconditionally stable method for calculation of time-dependent temperature fields. In other words, Eq 3-5 represent a discrete representation of drop-by-drop liquid-metal deposition, when diffusivity varies reasonably and monotonically as a function of position, that is unconditionally stable with respect to time-step size. With the general understanding of Eq 1-5 as an unconditionally stable discrete representation for calculation of temperature histories, the problem of establishing some assessment of error propagation as a function of time becomes of relevance.

At this stage, it is important to indicate that the classifications explicit and implicit, for discrete representations of the heat conduction equation, are motivated primarily by a direct-problem perspective for numerical modeling of physical processes. With respect to this perspective, the discrete representation Eq 3-5 can be applied for qualitative analysis of physical characteristics of a given drop-by-drop liquid-metal deposition process. This follows in that the calculated temperature field, although possibly not quantitatively accurate for relatively large time steps, is able to "shadow" the actual field to the extent that all qualitative trend features are preserved. This is a general characteristic of many implicit schemes. Accordingly, selection of an appropriate time-step size for qualitative accuracy can be verified by examination of the extent to which a calculated solution can shadow a physically consistent solution. This type of examination is exactly that represented by the calculated temperature histories shown in Fig. 3-5.

In principle, with respect to an inverse-problem perspective for numerical modeling of physical processes, the discrete representation Eq 2-5 can be applied for quantitative analysis of a given drop-by-drop liquid-metal deposition process. This follows in that the inclusion of Eq 2 provides an interesting property with respect to error propagation. Referring to Eq 2, one notes that the calculated temperature field, at any given time, can be "corrected" according to values of target temperatures T_n^c. It follows that by inclusion of Eq 2, which is with respect to an inverse-problem perspective, the discrete representation Eq 2-5 is equipped with a predictor-corrector property for calculating the time-dependent temperature field. In other words, any error propagation that is related to time-step size, tending to cause the calculated temperature field to deviate from its correct values, is corrected for within a specified tolerance $Z_T < \varepsilon$, at those times when Eq 2 is applied.

The predictor-corrector character of Eq 2-5, in terms of discrete representation, and convenient adjustability in terms of parametric representation, provides for the construction of process control algorithms: process control algorithms characterized by closed-loop feedback and control procedures for optimization with respect to specified temperature histories and alloy compositions. The general structure of these types of control algorithms is shown in Fig. 6. It can be noted from Fig. 6, that process control for the purpose of obtaining a specified temperature history, and thus a specified microstructure within a fabricated structure, requires minimization of two separate objective functions. One objective function is given by Eq 2, where the values of temperature T_n^c represent experimentally measured values of the temperature, which are typically

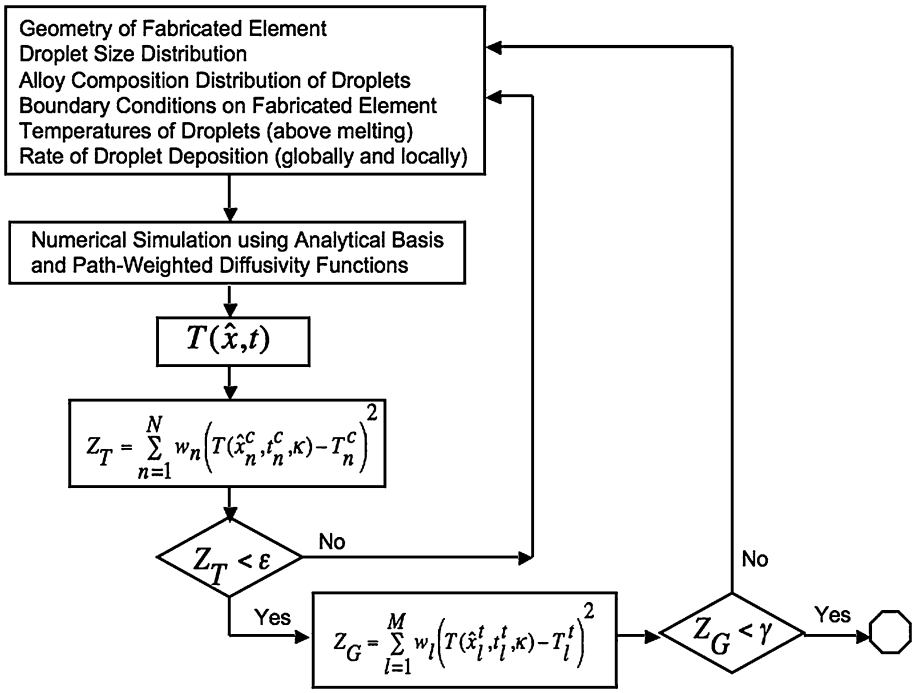

Fig. 6 General structure of process control algorithms for process control of drop-by-drop liquid metal deposition processes, where ε and γ are objective-function tolerances

distributed spatially at various positions on the surface of the fabricated structure. The other objective function is defined by

$$Z_{\mathrm{G}} = \sum_{l=1}^{M} w_l \left(T(\hat{x}_l^{\mathrm{t}}, t_l^{\mathrm{t}}, \kappa) - T_l^{\mathrm{t}} \right)^2 \qquad \text{(Eq 9)}$$

where T_l^{t} is the target temperature for position, $\hat{x}_l^{\mathrm{t}} = (x_l^{\mathrm{t}}, y_l^{\mathrm{t}}, z_l^{\mathrm{t}})$, which is typically within the volume of the fabricated structure. The values of the temperature T_l^{t} represent temperature histories corresponding to specific solid-state transformations. Referring to Fig. 6, the quantities ε and γ are tolerances for the objective functions Eq 2 and 9, respectively.

6. Conclusion

The objective of this article was to present a physically consistent path-weighted diffusivity function for parametric representation of heat diffusion patterns occurring within a volume of material where in there exists inhomogeneous or anisotropic thermal diffusivity. The parametric representation of heat diffusion, which is a functional of path-weighted diffusivity, follows from a specific definition of the inverse heat-transfer problem that permits flexibility with respect to process parameterization. This parametric representation can be interpreted in terms of discrete representations of the heat conduction equation for calculating time-dependent temperature histories. Further analyses are required for application of the basis function formalism defined by Eq 1-7 to inverse analysis of different types of drop-by-drop liquid-metal deposition, where thermal diffusivity is strongly dependent upon position. The adaptation of Eq 2-5 for process control of drop-by-drop liquid-metal deposition processes requires a consideration of parameter optimization procedures. Accordingly, the development of process control algorithms and associated parameter optimization procedures would be with respect to analysis of different types of drop-by-drop liquid-metal deposition processes and is therefore a subject for further study.

Acknowledgment

The authors thank the Office of Naval Research for providing support in performing this research.

References

1. K.P. Cooper, Layered Manufacturing: Challenges and Opportunities, *Mater. Res. Soc. Symp. Proc.*, 2003, **758**, p LL1.4.1
2. G.M. Fadel, S. Morvan, et al., *Solid Freeform Fabrication Proceedings*, University of Texas, Austin, TX, 2001, p 553
3. K.P. Cooper and S.G. Lambrakos, *Supplemental Proceedings, Vol 1, Fabrication, Materials, Processing and Properties*, TMS, Warrandale, PA, 2009, p 351
4. K.P. Cooper and S.G. Lambrakos, Thermal Modeling of Direct Digital Melt-Deposition Processes, *J. Mater. Eng. Perform.*, 2011, **20**(1), p 48–56
5. S.G. Lambrakos and K.P. Cooper, Path-Weighted Diffusivity Functions for Parameterization of Heat Deposition Processes, *J. Mater. Eng. Perform.*, 2011, **20**(1), p 31–39
6. S.G. Lambrakos and J.G. Michopoulos, Algorithms for Inverse Analysis of Heat Deposition Processes, *Mathematical Modelling of Weld Phenomena*, Vol 8, Verlag der Technischen Universite Graz, Austria, 2007, p 847–879
7. S.G. Lambrakos and J.O. Milewski, Analysis of Welding and Heat Deposition Processes Using an Inverse-Problem Approach, *Mathematical Modelling of Weld Phenomena*, Vol 7, Verlag der Technischen Universite Graz, Austria, 2005, p 1025–1055
8. H.S. Carslaw and J.C. Jaegar, *Conduction of Heat in Solids*, 2nd ed., Clarendon Press, Oxford, 1959, p 374
9. Sandia National Laboratories, *Advanced Metallurgy*, 2007, https://share.sandia.gov/8700/projects/content.php?cid=50
10. S.V. Patankar, *Numerical Heat Transfer and Fluid Flow*, Hemisphere Publishing, New York, 1980